Lab on a Chip

Cite this: *Lab Chip*, 2012, **12**, 1378

www.rsc.org/loc

PAPER

Pulsed laser triggered high speed microfluidic fluorescence activated cell sorter†‡

Ting-Hsiang Wu,[ab] Yue Chen,[a] Sung-Yong Park,[a] Jason Hong,[b] Tara Teslaa,[b] Jiang F. Zhong,[c] Dino Di Carlo,[d] Michael A. Teitell[b] and Pei-Yu Chiou*[a]

Received 8th November 2011, Accepted 9th February 2012
DOI: 10.1039/c2lc21084c

We report a high speed and high purity pulsed laser triggered fluorescence activated cell sorter (PLACS) with a sorting throughput up to 20 000 mammalian cells s^{-1} with 37% sorting purity, 90% cell viability in enrichment mode, and >90% purity in high purity mode at 1500 cells s^{-1} or 3000 beads s^{-1}. Fast switching (30 μs) and a small perturbation volume (~90 pL) is achieved by a unique sorting mechanism in which explosive vapor bubbles are generated using focused laser pulses in a single layer microfluidic PDMS channel.

Introduction

Microfluidic-based fluorescence activated cell sorters (μFACS) have several advantages over conventional electrostatic-droplet-based cell sorters. A closed detection and sorting environment prevents aerosols that can potentially contaminate equipment, personnel, and subsequent sorting experiments. This advantage is critical when sorted cells are re-cultured or used for PCR analysis as the contaminant can be exponentially expanded, resulting in artifacts.[1] Micrometre-sized channel dimensions are also suitable for handing small sample volumes and low cell numbers with high yield.[2] Microfluidic sorting chips can be made disposable, which offers improved biosafety for sorting pathogenic samples. Furthermore, additional functionalities such as population expansion,[3] drug screening,[4] single-cell DNA[5] and RNA[6] analyses can be integrated directly downstream of the sorting region on the same chip, minimizing sample loss and time delay between sorting and subsequent processes. Although various on-chip μFACS mechanisms have been demonstrated, sorting live mammalian cells at high speeds with high sort purity and cell viability remains a challenge. By using electro-osmotic flow switching, *E. coli* cells were sorted at 20 cells s^{-1}.[7] An integrated microfabricated PDMS valve[8] demonstrated a sorting speed of 44 cells s^{-1}. By dynamically plugging the channel with a thermo-reversible gelation polymer,[9] sorting of *E. coli* was shown at 5 cells s^{-1}. Using optical force routing,[2] high sort purities >90% was achieved with HeLa cells at a sorting speed of ~100 cells s^{-1}. Under the enrichment mode of sorter operation, a throughput of 12 000 cells s^{-1} was demonstrated using an off-chip flow switching valve but with a low sorted purity of 0.2%.[10] Alternatively, an enrichment of ~230-fold (sort purity ~65%) at 1000 mammalian cells s^{-1} was reported using an integrated piezoelectric actuator (PZT)-driven polydimethylsiloxane (PDMS) membrane valve.[11] Slow cell switching mechanisms and large fluid perturbation volumes are the two major factors limiting the throughput and purity of current microfluidic FACS devices. Reported switching times range from 500 msec using dielectrophoretic force switching,[12] 3 msec using flow switching with a thermo-reversible gelation polymer[9] or with optical force swithcing,[2] and 0.1 msec for the PZT-driven membrane valve.[11] These mechanisms are orders of magnitude slower than the speed of standard electrostatic-droplet-based cell sorters. Microfluidic based droplet sorters[13] on the other hand demonstrated 0.5 msec switching time with speeds up to 2000 droplets s^{-1}. A faster cell sorting rate is limited by droplet breakage and cell encapsulation efficiency. Two-phase (aqueous droplets in an oil medium) systems also increase the complexity in subsequent cell recovery and processing. A micromachined, silicon-based bubble jet sorter showed switching of microspheres at 4.9 μs switching time.[14] However, sorting of mixed populations of live cells has not been demonstrated.

Pulsed laser microbeams have been shown to induce bubble cavitation in solution on the microscale for high-speed droplet

[a]*Department of Mechanical and Aerospace Engineering, University of California, Los Angeles (UCLA), 420 Westwood Plaza, Rm 37-138, Los Angeles, CA, 90095, USA. E-mail: pychiou@seas.ucla.edu; Tel: +1-310-825-8620*

[b]*Department of Pathology and Laboratory Medicine, UCLA, Los Angeles, CA, 90095, USA. E-mail: mteitell@mednet.ucla.edu; Fax: +1-310- 267-0382; Tel: +1- 310- 206-6754*

[c]*Department of Biochemistry and Molecular Biology, University of Southern California, 2011 Zonal Avenue, HMR 308, Los Angeles, CA, 90033, USA. E-mail: jzhong@usc.edu; Tel: +1- 323- 442-2371*

[d]*Department of Bioengineering, UCLA, 420 Westwood Plaza Rm 5121 ENG V, Los Angeles, CA, 90095, USA. E-mail: dicarlo@seas.ucla.edu; Tel: +1-310- 983-3235*

† Electronic supplementary information (ESI) available. See DOI: 10.1039/c2lc21084c

‡ Author contributions: T.W., J.F.Z., D.D., M.A.T. and P.C. designed the research; T.W., Y.C. and S.P. fabricated the device and performed sorting experiments; T.W. and T.T. conducted flow cytometry analyses; and J.H. performed mRNA analyses. All authors contributed to writing the paper.

generation,[15] enhancing fluid mixing,[16] microfluidic switching,[17] and gene transfection.[18] When a laser pulse with energy surpassing a threshold is focused in a liquid medium (*e.g.* water), the intense optical field generates heated plasma within the focal volume. The sharp temperature increase and thermoelastic stress built-up induces a cavitation bubble at the laser focus within nanoseconds. The bubble lifetime and bubble volume are determined by the laser wavelength, laser fluence at the focal spot, and pulse duration.

Here we demonstrate a microfluidicbased, high-speed and high-purity pulsed laser activated cell sorter termed PLACS which utilizes small volume liquid jets induced by pulse laser triggered cavitation bubbles for sample switching. A complete switch cycle in PLACS, as characterized by the bubble lifetime, is 30 μs. Bubble expansion and collapse transiently switches fluid flow inside the microchannels. The actuated fluid volume and the actuation location can be precisely controlled by the deposited laser pulse energy and laser focus position. By using all optical switching and eliminating any on-chip active components, the microfluidic chip is made of a single-layer PDMS channel bonded to a glass cover slide, which can be low cost and disposable. Furthermore, PLACS is compatible with the vast repertoire of PDMS-based microfluidic structures for performing additional upstream or downstream functions and analyses.

Principle of PLACS

The design of PLACS is depicted in Fig. 1a. The microfluidic chip consists of a main channel with two outlets, collection and waste. The pulsed channel runs in parallel with the main channel and is connected to the main channel through a straight narrow nozzle at the tip of the Y junction. Using hydrodynamic focusing, the input samples are focused to a narrow stream and flow into the left waste outlet. As a desired object flows through the fluorescence detection region upstream of the Y junction, a laser pulse is triggered and focused through a high NA objective lens into the pulsed channel after an optimal delay time. This induces an explosive cavitation bubble which expands and displaces the surrounding fluid creating a high speed liquid jet through the nozzle into the main channel. This liquid jet deflects the desired object into the collection channel. A rapid switching cycle of 30 μs is demonstrated based on the expansion and collapse rate of a cavitation bubble (Fig. 2). Using a nozzle to focus the deflecting liquid jet narrows the switching region in the sample stream and minimizes the disturbance range on neighboring objects to 60 μm (Fig. 3). This is essential for achieving high throughput and high sorting purity. Previously, we demonstrated that a laser-induced cavitation bubble can deform an elastic membrane for switching an adjacent fluid or particle flow.[17] In that prior case, the membrane deformation extended over hundreds of microns in length, which perturbed a large fluid volume and affected sample flows upstream of the switching region, yielding lower sort purity. In this work, the volume of liquid jet delivered into the sample channel as captured by the time resolved image is ~90 pL (Fig. 2 at 15 μs). Combined with the capability of operating at high sample flow speeds of ~1 m s^{-1}, PLACS can achieve mammalian cell sorting at high speeds with high purities.

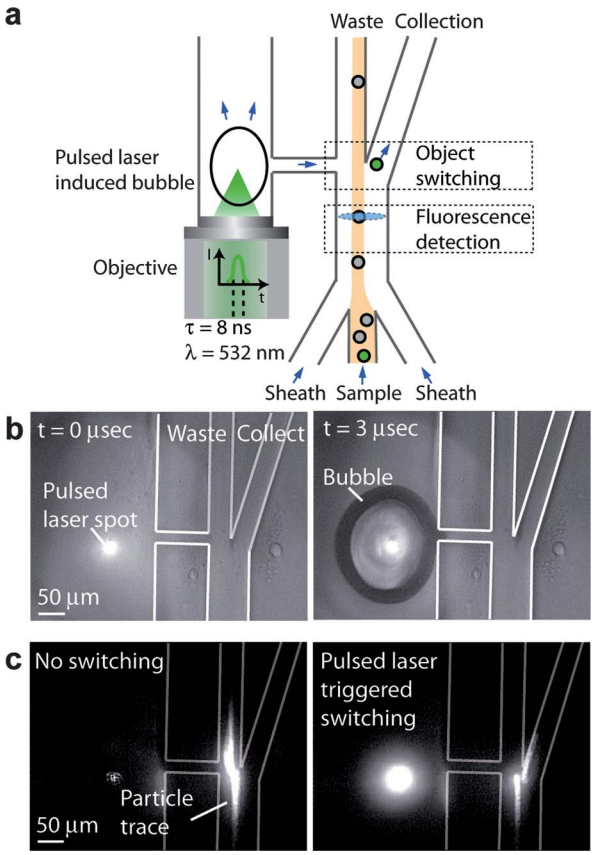

Fig. 1 PLACS operation. (a) Schematic of the cell sorter. The sample flow is hydrodynamically focused into the waste channel. As the desired objcet flows through the fluorescence detection region upstream form the Y junction, the laser puls is triggered after an optimum delay and induces a cavitation bubble in the adjacent pulsed channel. The bubble expansion produces a high-speed liquid jet that deflects the desired sample towards the collection channel for sorting. (b) Time-resolved images of the cavitation bubble generated by the focused pulsed laser beam in the microfluidic cell sorter. (c) Fluorescent particle switching in PLACS. Without switching, the particle flows towards the left waste outlet. With fluorescence activated switching, a laser pulse was triggered and the particle was sorted into the collection outlet on the right.

Materials and methods

Experiment setup and device fabrication

As shown in Fig. 4, the pulsed laser system was a Q-switched Nd:YVO_4 laser (EKSPLA, Jazz 20) operating at 532 nm wavelength, 8 ns pulsewidth, and a repetition rate up to 100 kHz. The pulsed laser beam was expanded and focused by an objective lens (100×, NA 0.9) through the glass substrate into the pulsed channel. The laser focus was positioned 100 μm away from the connection nozzle to the main channel. The laser pulse energy deposited into the channel was adjusted using a half-wave plate followed by a polarizing beam splitter and was set at 31 μJ per pulse for switching. For sample fluorescence excitation, a 10 mW, 488 nm solid state laser (CyrstaLaser, DL-488-010) was reflected by a dichroic mirror (Chroma, z488rdc) and lightly focused into the main channel through a 25×, NA 0.4 objective lens from the PDMS side of the microfluidic chip. The emitted sample fluorescence was collected by the same objective lens

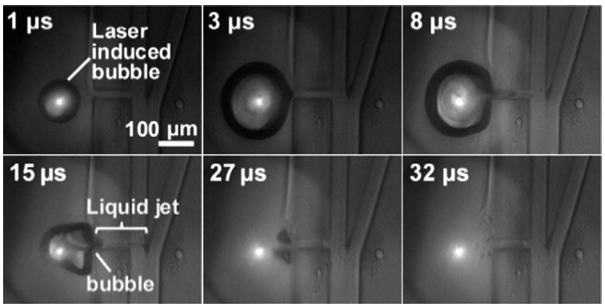

Fig. 2 A cavitation bubble was generated within nanoseconds after laser pulse arrival. The bubble grew to a maximum diameter of 230 μm in the major axis and 205 μm in the minor axis within 3 μs and began to collapse. During bubble expansion, the surrounding fluid was displaced at the speed of the bubble front and a high-speed liqued jet was induced in the connecting nozzle into the main sample channel, deflecting the targeted object towards the collection channel. The liqued injected into the sample channel is 140 μm (liquid jet length) × 20 μm (nozzle width) × 30 μm (channel height) ~90 pL (see 15 μs). The bubble collapsed completely by 30 μs after the laser pulse. Allura Red dye (concentration 67 mg ml^{-1}, Sigma-Aldrich) was added in the pulsed channel flow. Laser pulse energy was 31 μJ.

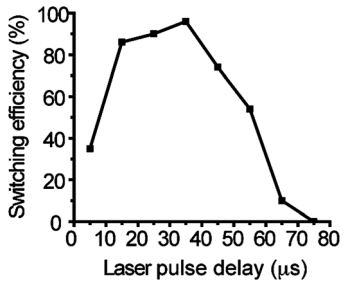

Fig. 3 Switching window and optimum object switching delay. Particle switching efficiency was measured at different laser pulse delays ranging from 5 to 75 μs after detection. The highest switching efficiency of 96% was obtained at a delay of 35 μs and decreased to 0% at 75 μs. The perturbation range of neighboring objects is ~60 μm, estimated by the particle speed (0.8 m s^{-1}) and the 75 μs window. The distance between the detection region and Y junction was 50 μm. The sorting efficiency was obtained by analyzing particle traces from 50 switching events for each delay condition.

and detected using a photomultiplier tube (Sens-Tech, P30CWAD5-01) after passing through a bandpass filter (Chroma, HQ510/20m) matching the fluorescence emission spectrum. An aperture preceded the PMT and was placed at the sample conjugate image plane. The aperture opening defined the fluorescence detection area to be ~30 × 80 μm covering the entire width of the sample channel and blocked scattered light from the laser pulse and plasma emission. The PMT signal was integrated using a DAQ card (National Instruments, PCI 7831R) at 100 kHz. FPGA logic was programmed using LabView (National Instruments) to perform real-time detection, threshold comparisons, and timed triggering of the pulsed laser. To image and characterize the fast dynamics of the cavitation bubble, a flashlamp (High-Speed Photo-Systeme, Nanolite KL-M) with 11 ns flash duration was used as the illumination for time-resolved photography. Images were taken by a CCD camera (Zeiss, AxioCam MRm) and the flash delay from the laser pulse was controlled by LabView.

The device was fabricated using a conventional replica molding technique.[19] Microchannel features were photolithographically defined in SU-8 (MicroChem 2025) photoresist molds on a silicon wafer and then replicated onto a PDMS (Sylgard 184) layer. The PDMS replica was bonded to a glass cover slide substrate after oxygen plasma treatment. The measured microchannel height was 30 μm. Sheath flow channels were 80 μm wide. The sample channel width was 80 μm, which separated into 40 μm wide collection and waste outlet channels at the Y junction. The pulsed channel width was 300 μm and the straight nozzle connecting the sample and pulsed channel had a channel width of 20 μm and length of 100 μm.

Sorting of microbeads and mammalian cells

For particle sorting experiments, 10 μm green fluorescent beads (Thermo Fisher Scientific, G1000) and 10 μm non-fluorescent beads (Polysciences, 17136-5) were suspended in deionized water with 3% w/v Tween 80 (Sigma-Aldrich) to the desired concentrations. Sheath flows contained deionized water with 3% w/v Tween 80. All channel flows were driven by syringe pumps (Harvard Apparatus, PHD2000). Allura Red dye (concentration 67 mg ml^{-1}, Sigma-Aldrich) was added in the pulsed channel flow

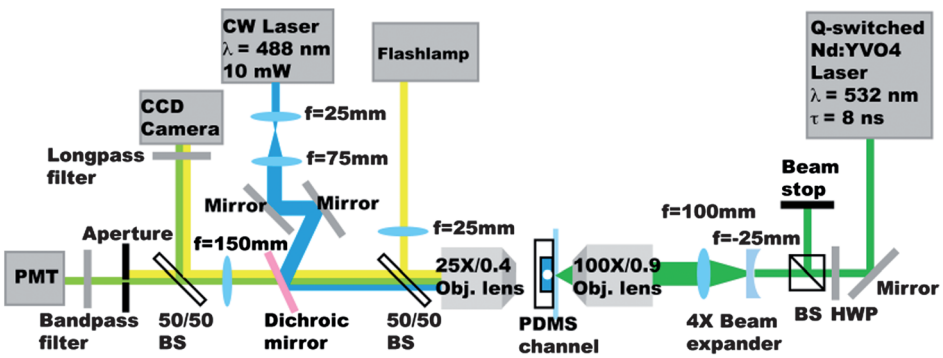

Fig. 4 PLACS experimental setup. For cavitation bubble induction, we used a Q-switched, 8ns pulsewidth Nd:YVO4 laser. The pulsed laser beam was focused by an objective lens (100×, NA 0.9) into the pulsed channel. Sample fluorescence was detected by a photomultiplier tube and sampled using a DAQ card and integrated every 10 μs. FPGA logic was programmed using LabView to perform real-time detection, threshold comparison and timed triggering of the pulsed laser.

to reduce the laser energy threshold for bubble generation. The sample flow rate was 1.2 ml h^{-1} and the average sample speed was 0.8 m s^{-1} in the main channel. For cell sorting, human Nalm-6 pre-B cells or B lymphoma Ramos cells cultured in RPMI 160 culture media with usual supplements were washed and re-suspended in phosphate buffered saline (1x PBS, pH 7.4) with 2% w/v bovine serum albumin (BSA) to the desired concentration. Fluorescent cell samples were obtained by staining Nalm-6 or Ramos cells with Calcein AM (Invitrogen). After sorting, the collected cells were incubated at 37 °C, 5% CO_2 for 30 min in PBS before addition of propidium iodide (Invitrogen) for viability evaluation. The sample flow rate and flow speed settings were the same as the particle sorting experiments.

Sort purity analyses by flow cytometry

Sorted samples purities were analyzed by a flow cytometer (BD, FACSCantoII). Positive and negative control samples were used to configure the fluorescence gating conditions. For each sort condition, the average sort purity was obtained from measurements of 3 experiments. In each measurement, the total number particles analyzed were ~5000. Cell viability based on propidium iodide exclusion was measured on the same flow cytometer with a sample size of ~5000 cells for each sorting experiment.

Gene expression quantification

Human Nalm-6 pre-B cells were suspended in sorting buffer (1x PBS, pH 7.4, with 2% w/v BSA) to a concentration of ~1 × 10^6 ml^{-1}. The mixture ratio of Calcein-AM stained cells *versus* unstained cells was 1 : 1. Cells were sorted through PLACS at room temperature and sorted cells were retrieved from both the collection and waste outlets (~1 × 10^6 cells in each sample). Unsorted cells were incubated in sorting buffer at room temperature for the same duration as the sorted cells. RNA was extracted from retrieved cells immediately after sorting using the RNeasy Mini Kit (Qiagen) following the manufacturer's protocols. Real-time qPCR was performed according to manufacturer's protocol on the Roche LightCycler 480 Real-Time PCR System with SYBER Green I Master mix (Roche). For base level gene expression evaluation, cells were incubated in culture media at 37 °C, 5% CO_2 before mRNA extraction. For positive controls, Nalm-6 cells were incubated in media at 42 °C for one hour for *HSPA6* evaluation, whereas for *FOS* evaluation, cells were treated with 10 μg ml^{-1} cycloheximide (Sigma-Aldrich) for two hours. Primers for gene expression were generated using Roche's Universal Probe Library Assay Design Center online.

FOS (*c-fos*) Fwd: (CTACCACTCACCCGCAGACT)
Rev: (AGGTCCGTGCAGAAGTCCT).
HSPA6 Fwd: (TCATGAAGCCGAGCAGTACA)
Rev: (GTTTTTGGCAGCCACTCTGT).
GAPDH Fwd: (GCTCTCTGCTCCTCCTGTTC)
Rev: (ACGACCAAATCCGTTGACTC).

Results and discussion

Bubble dynamics and fluid perturbation volume estimation

In PLACS, once a desired object was detected, a nanosecond laser (532 nm wavelength, 8 ns pulsewidth) induced a bubble that expanded to a maximum diameter (major axis) of 230 μm in 3 μs after laser pulse arrival (Fig. 1b). Fig. 1c shows a fluorescent particle trace that was successfully switched into the collection outlet on the right by a pulsed laser triggered high speed bubble flow. Perturbation volume was estimated by measuring the maximum liquid jet volume injected into the main sample channel. As captured by time-resolved imaging, the liquid jet flow reached the center of the main sample channel while the bubble front reached the boundary of the pulsed channel (Fig. 2, 15 μs). Estimated liquid jet volume is 140 μm (liquid jet length) × 20 μm (nozzle width) × 30 μm (channel height) ~90 pL.

Switching window characterization and optimizing object switching delay after detection

The switching window or perturbation range was determined by measuring particle switching efficiency at different time delays after detection. Particles were detected at a distance of 50 μm upstream of the "Y" junction. Switching efficiency was measured for particles at different locations with respect to the nozzle (translating to different time delays after detection) as the laser pulse was triggered. The highest efficiency was 96% obtained at a delay of 35 μs and the efficiency decreased to 0% at a delay of 75 μs and <40% at 5 μs (Fig. 3). Particles outside of this region (75 μs × particle speed 0.8 m s^{-1} = 60 μm) were not switched and followed the original flow focusing streamline into the waste channel. The switching window and optimal delay time between triggering laser pulsing for switching and object detection depend on the sample flow speed and the detection region distance to the Y junction. Variable delay time between object detection by the PMT and laser triggering was controlled by FPGA programmed in LabView (see Experimental setup section). For different delay times ranging from 5 to 75 μs, fluorescent particle traces were recorded and analyzed. Switching efficiency was obtained by measuring the percentage of successful switching events (particle trace going into the collection channel) in a total of 50 sampled fluorescent particle images.

Sorting of mixed polystyrene microspheres

We characterized the sorter performance at different object throughputs and initial mix ratios. Samples were prepared by mixing 10 μm green fluorescent beads with non-fluorescent polystyrene beads. Throughputs ranging from 3000 to 10 000 particles/s were obtained by keeping the green bead concentration at 5.7 × 10^4 ml^{-1} while increasing the non-fluorescent bead concentration accordingly. High purities (>90%) of the sorted beads were obtained at a sorting throughput of 3000 particles s^{-1} by analyzing the collection sample using a commercial flow cytometer (Fig. 5a,b and Supplementary Movie 1). The fluorescent beads were enriched from an initial mix ratio of 0.0087 to a final ratio of 9.61, corresponding to a 1105-fold enrichment. At higher throughputs the sort purity decreases as a result of the narrowing of the average distance between adjacent particles (Fig. 5c). At a throughput of 10 000 particles s^{-1} the collection purity was 45%, equivalent to a 426-fold enrichment. To evaluate sorter performance in switching individual particles at high frequencies compared to rare event sorting, bead samples with initial mix ratios ranging from 0.01 to 0.27 (unsorted purity

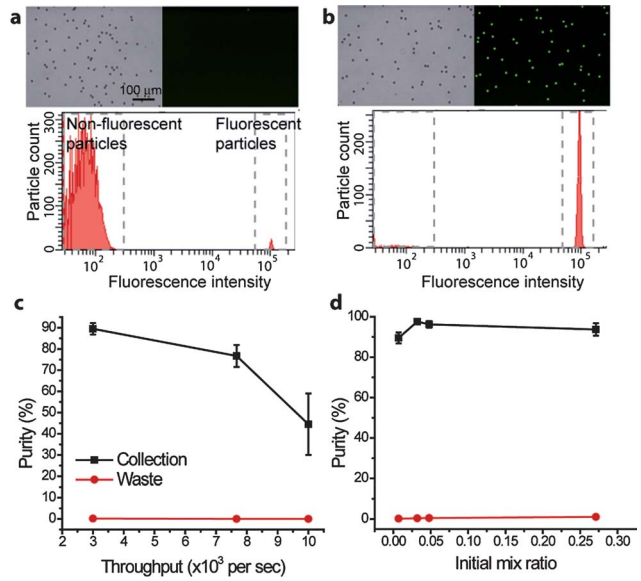

Fig. 5 PLACS sorting results. (a) Mixed 10 μm green fluorescent and non-fluorescent polystyrene microspheres before sorting. Initial mix ratio = 0.0087. (b) Collected sample after sorting with a final mix ratio = 9.61. Fluorescent microsphere concentration was enriched by a factor of 1105. (c) Sort purity at different sorting speeds ranging from 3000 to 10 000 microspheres s^{-1}. High purities (90 ± 3% (mean ± s.d.)) of the sorted particles were obtained at a sorting throughput of 3000 particles s^{-1}. The collection purity measured at the highest speed tested (10 000 particles s^{-1}) was 45 ± 15%. The sort purity decreased at higher throughputs as the average distance between adjacent particles shortened. In these experiments, green fluorescent particle concentrations were kept constant (5.7×10^4 ml^{-1}) while non-fluorescent particle concentrations were increased accordingly to obtain the target throughput. (d) Sort purity at different initial mix ratios ranging from 0.001 to 0.27 (unsorted purity 1% to 21%). At the initial mix ratio of 0.27, measured collection target particle purity was 94 ± 3% and waste target particle purity was 1 ± 0%. Sorting speed was kept at 3000 particles s^{-1}.

1% to 21%) were sorted at a throughput of 3000 particles s^{-1}. High collection object purity (94%) with low target object waste (1%) were maintained even at the highest initial mix ratio tested.

Sorting of mammalian cells

To evaluate mammalian cell sorting, human pre-B Nalm-6 or B lymphoma Ramos cells were stained with calcein AM (green fluorescence) and mixed with untreated cells at the desired ratios. Results showed at sorting speeds of 560 and 1500 cells s^{-1}, >90% purity with ~90% cell viability were obtained for sorting fluorescent Nalm-6 cells (Table 1), a performance comparable to similar experiments performed on a high-end commercial FACS.[11] For high-speed cell enrichment, Ramos cells were sorted at 10 000 cells s^{-1} and 20 000 cells s^{-1}. The obtained sort purities were 48.6% and 37.4%, corresponding to enrichment factors of 473 and 298.5 respectively (Table 1). Under these sorting conditions, cells sorted into the collection or waste channels exhibited the same stress levels seen in unsorted cells, as measured by *HSPA6* and *FOS* stress-response gene expression[2] (Fig. 6). These results showed that hydrodynamic cell focusing and cavitation bubble triggered liquid jet switching did not exert additional stress on the cells being sorted.

Device reliability

The reproducibility of PLACS sorting process under repeated laser pulsing and bubble cycles was tested. We verified that the microchannels remained intact and exhibited no burning or leakage after 100 million (10^8) actuations (Fig. 7). Cavitation bubbles after 100 million cycles showed no discernible changes in

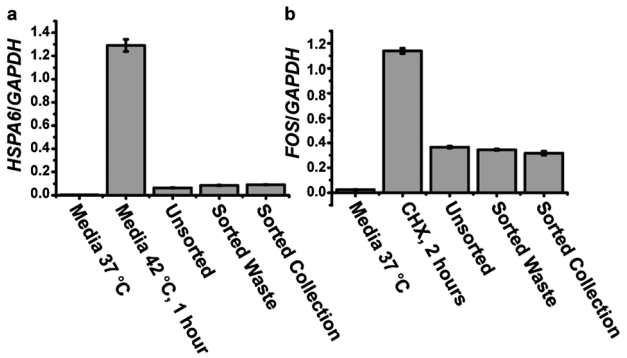

Fig. 6 Evaluation of stress levels of Nalm-6 cells after PLACS sorting. (a,b) The *HSPA6* gene expression level indicates the cellular response to heat shock, and *FOS* gene expression reflects heat shock and fluidicshear stress. Gene expression levels were normalized to a GAPDH housekeeping gene for all cell samples under different conditions. Sorted cells retrieved from the collection and waste outlets showed expression levels that were statistically similar to the unsorted cells (incubated in sorting buffer at room temerature for the sort duration). A positive control for *HSPA6* expression was provided by incubationg Nalm-6 cells in culture media at 42 °C for one hour. For *FOS* expression, a positive control was provided by treating Nalm-6 cells with cycloheximide (CHX) for two hours.

Table 1 Results of sorting Nalm-6 human pre-B cells and B lymphoma Ramos cells at different sorting throughputs (Col: Collection sample; W: Waste sample)

		Before sort			After sort			
Throughput (cells s^{-1})	Cell Type	Initial green cell percentage (%)	Cell density ($\times 10^6$ cells ml^{-1})	Viability (%)	Col. purity (%)	W. purity (%)	Col. viability (%)	W. viability (%)
560	Nalm-6	1.2	1	94.1	91.5	0.3	90	84.4
1500	Nalm-6	0.8	4.6	93.4	97.9	0.3	89.4	90.2
10 000	Ramos	0.2	30.6	98	48.6	0.1	87.6	97
20 000	Ramos	0.2	61.3	98.5	37.4	0.0	98.8	98.1

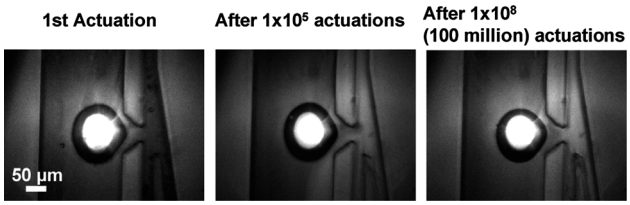

Fig. 7 PLACS reliability evaluation. A laser-induced cavitation bubble (imaged at 3 μs after laser pulse arrival) could be repeatedly produced >100 million times without showing significant bubble pattern alteration or microchannel degradation. The pulsed laser repetition rate was 10 kHz.

the bubble pattern, further ensuring reliable switching over long periods of device operation.

Conclusion

PLACS overcomes the limit of microfluidic-based fluorescence-activated cell sorting mechanisms in achieving simultaneously high speed, high purity, and high viability sorting. The bubble jet switching mechanism actuates a small and well-controlled fluidic volume for sample sorting which allows sorting of multiple cell types in any biological medium. Our current device operates with a bubble cycle time of 30 μs. Shorter switching times are possible by utilizing a smaller bubble actuation volume and modified channel design. PLACS has the potential to bridge the sorting throughput gap between current microfluidic FACS and conventional electrostatic-droplet-based cell sorters.

Acknowledgements

The authors thank Dr Kayvan Niazi and Dr Shahrooz Rabizadeh (California NanoSystems Institute) for helpful discussions and support. This work was supported in part by NSF ECCS-0901154, NSF DBI-0852701, NIH R21EB014456, a UC Discovery/Abraxis BioScience Biotechnology Award (#178517), and by the Broad Center of Regenerative Medicine and Stem Cell Research at UCLA. We thank the UCLA Nanoelectronics Research Facility and Center for Cell Control for providing instrumentation for device fabrication and characterization.

References

1 L. W. Arnold and J. Lannigan, Practical issues in high-speed cell sorting, *Curr. Protoc. Cytom.*, 2010, **1**, 1.24.21–21.24.30.
2 M. M. Wang, *et al.*, Microfluidic sorting of mammalian cells by optical force switching, *Nat. Biotechnol.*, 2005, **23**, 83–87.
3 L. Kim, M. D. Vahey, H.-Y. Lee and J. Voldman, Microfluidic arrays for logarithmically perfused embryonic stem cell culture, *Lab Chip*, 2006, **6**, 394–406.
4 P. S. Dittrich and A. Manz, Lab-on-a-chip: microfluidics in drug discovery, *Nat. Rev. Drug Discovery*, 2006, **5**, 210–218.
5 M. B. Elowitz, A. J. Levine, E. D. Siggia and P. S. Swain, Stochastic gene expression in a single cell, *Science*, 2002, **297**, 1183–1186.
6 J. Zhong, *et al.*, A microfluidic processor for gene expression profiling of single human embryonic stem cells, *Lab Chip*, 2008, **8**, 68–74.
7 A. Y. Fu, C. Spence, A. Scherer, F. H. Arnold and S. R. Quake, A microfabricated fluorescence-activated cell sorter, *Nat. Biotechnol.*, 1999, **17**, 1109–1111.
8 A. Y. Fu, H.-P. Chou, C. Spence, F. H. Arnold and S. R. Quake, An integrated microfabricated cell sorter, *Anal. Chem.*, 2002, **74**, 2451–2457.
9 K. Ozaki, *et al.*, Microfluidic cell sorter with flow switching triggered by a sol–gel transition of a thermo-reversible gelation polymer, *Sens. Actuators, B*, 2010, **150**, 449–455.
10 A. Wolff, *et al.*, Integrating advanced functionality in a microfabricated high-throughput fluorescent-activated cell sorter, *Lab Chip*, 2003, **3**, 22–27.
11 S. H. Cho, C. H. Chen, F. S. Tsai, J. M. Godin and Y.-H. Lo, Human mammalian cell sorting using a highly integrated micro-fabricated fluorescence-activated cell sorter (μFACS), *Lab Chip*, 2010, **10**, 1567–1573.
12 D. Holmes, M. E. Sandison, N. G. Green and H. Morgan, On-chip high-speed sorting of micron-sized particles for high-throughput analysis, *IEE Proc.: Nanobiotechnol.*, 2005, **152**, 129–135.
13 J.-C. Baret, *et al.*, Fluorescence-activated droplet sorting (FADS): efficient microfluidic cell sorting based on enzymatic activity, *Lab Chip*, 2009, **9**, 1850–1858.
14 C. Chen, J. Wang and O. Solgaard, Micromachined bubble-jet cell sorter with multiple operation modes, *Sens. Actuators, B*, 2006, **117**, 523–529.
15 S.-Y. Park, T.-H. Wu, Y. Chen, M. A. Teitell and P.-Y. Chiou, High-speed droplet generation on demand driven by pulse laser-induced cavitation, *Lab Chip*, 2011, **11**, 1010–1012.
16 A. N. Hellman, *et al.*, Laser-Induced mixing in microfluidic channels, *Anal. Chem.*, 2007, **79**, 4484–4492.
17 T.-H. Wu, L. Gao, Y. Chen, K. Wei and P.-Y. Chiou, Pulsed laser triggered high speed microfluidic switch, *Appl. Phys. Lett.*, 2008, **93**, 144102.
18 U. K. Tirlapur and K. König, Targeted transfection by femtosecond laser, *Nature*, 2002, **418**, 290–291.
19 Y. Xia and G. M. Whitesides, Soft lithography, *Angew. Chem., Int. Ed.*, 1998, **37**, 550–575.